

Spin-wave calculations for multilayered structures

Burkard Hillebrands

2. *Physikalisches Institut, Rheinisch-Westfälische Technische Hochschule,
5100 Aachen, Federal Republic of Germany*

(Received 29 June 1989)

Results are presented on the calculations of spin-wave frequencies in ferromagnetic layers, double layers, and multilayered structures for small, nonzero wave vectors such as can be investigated by, e.g., Brillouin light scattering. The underlying continuum-type magnetostatic theory includes both dipolar and exchange contributions and fully takes into account magnetic surface and interface anisotropies as well as interlayer exchange coupling. For single magnetic layers the detailed influence of surface anisotropies on both film surfaces is studied. For magnetic double layers the interlayer exchange coupling mechanism is investigated. In the case of multilayers consisting of alternating magnetic and nonmagnetic layers, the crossing regime between dipolar and exchange modes shows a strong dependence of the gap width on the amount of interface anisotropy. For small layer thicknesses the interlayer exchange coupling shifts the spin-wave frequencies of all but the highest-frequency dipolar modes into the exchange-mode regime. In the case of all-magnetic multilayered structures, a new type of collective spin-wave excitations arising from coupled exchange modes is predicted.

I. INTRODUCTION

Spin waves in layered magnetic structures have spurred interest both because of the growing technological importance of these kinds of materials, as well as the advent of new experimental techniques, which makes experimental access to properties of magnetic excitations easier. There are basically two types of magnetic excitations that play an important role in layered magnetic structures. Long-wavelength dipolar excitations (so-called Damon-Eshbach modes) exist on each magnetic layer. These modes can be coupled via their dipolar stray fields to form a set of collective magnetostatic spin-wave excitations in magnetic multilayers. In addition, small-wavelength spin-wave modes determined primarily by magnetic exchange exist in magnetic layers. The wave vector of these modes is determined mainly by the layer thickness.

A well-developed method for studying spin-wave excitations is ferromagnetic resonance (FMR). Many of the basic properties of spin-wave propagation in thin films and multilayers have been studied by FMR, and basic concepts of magnetic coupling mechanisms have been developed in view of available FMR data. However, apart from situations where nonzero wave vectors are introduced through finite-geometry effects, FMR is restricted to dipolar zero-wave-vector spin-wave excitations (uniform modes). An example of a nonzero wave-vector situation are the so-called standing spin waves, i.e., exchange-dominated modes with the wave vector determined by layer thickness. The intrinsic lack of finite-wave-vector excitations results in a separation of dipolar-type spin-wave excitations (uniform modes) and exchange excitations (standing spin waves) in an appropriate theoretical description. However, the cross-over regime of dipolar modes and exchange modes is not

accessible with FMR.

On the other hand, Brillouin light scattering offers a versatile experimental tool to study nonzero wave-vector spin-wave excitations in magnetic structures. The wave vector of detected spin waves is determined by the momentum transfer from light to spin waves in the inelastic light scattering process. Using Brillouin light scattering, the collective dipolar spin-wave excitations in magnetic multilayers could be observed experimentally for the first time. Dipolar collective modes exhibit their unique properties only for nonzero wave vectors; they degenerate in an FMR experiment. Because of nonzero wave vectors, dipolar modes contain a small but measurable admixture of exchange character. There is a cross-over regime of dipolar-type modes and exchange-type modes, where both modes mix their character, showing characteristic mode repulsions. These effects, and many more, can be studied easily using Brillouin light scattering.

Although a large amount of Brillouin light scattering work exists for bulk materials and for single magnetic layers, there have been only a few theoretical or experimental studies of Brillouin light scattering in multilayered structures and superlattices. The first calculations, restricted to the dipolar limit, were reported by Camley, Rahman, and Mills,¹ Grünberg and Mika,² Emtage and Daniel,³ and, including volume anisotropy contributions, by Rupp, Wettling, and Jantz.⁴ This early work neglected exchange contributions as well as the possible influence of magnetic interface anisotropies on the spin-wave modes. Exchange modes in multilayers have been considered by van Staple *et al.*,⁵ Dobrzynski *et al.*,⁶ Albuquerque *et al.*,⁷ Hinchey and Mills,⁸ Vayhinger and Kronmüller,^{9,10} and Barnás.¹¹

However, very little attention has been directed toward interface anisotropies. Although these authors were able

to predict the salient features of the new collective spin-wave excitations in superlattices, recent Brillouin light scattering experiments by Hillebrands *et al.*^{12,13} show the effect of interface anisotropies for small layer thicknesses, as demonstrated for Fe/Pd superlattices. Experimental evidence for spin-wave modes in magnetic double layers has been reported by Grünberg and co-workers,^{14–16} Heinrich *et al.*,¹⁷ Cochran and Dutcher,¹⁸ and for multilayered structures by Grimsditch, Khan, and Schuller for Mo/Ni superlattices.¹⁹ A detailed experimental proof of the predicted magnetic properties of the collective spin-wave excitations was presented by Hillebrands *et al.*¹³

In this paper theoretical investigations applicable to Brillouin light scattering experiments are presented on the properties of spin waves in layered ferromagnetic structures. We do not use Bloch's theorem, but instead calculate the spin-wave modes for finite numbers of layers, since this approach bears more relevance to forthcoming experimental investigations. The calculations are based on single-layer calculations performed by Rado and Hicken²⁰ and by Cochran and Dutcher,²¹ and are extended towards double layers and multilayered structures. Preliminary results have been published in a preceding Rapid Communication.²² Multilayers consisting of alternating magnetic and nonmagnetic layers (magnetic/nonmagnetic multilayers) as well as all-magnetic multilayered structures are considered. The model includes both dipolar and exchange interactions as well as volume and interface anisotropy contributions, and is applied to a variety of layered magnetic structures.

The paper is organized as follows. In Sec. II the basic theoretical considerations are outlined. In Sec. III the theory is applied to single magnetic layers and some remarks are added to existing work on spin waves in magnetic films. Section IV presents the results for magnetic double layers and discusses the role of interlayer exchange coupling. In Sec. V magnetic/nonmagnetic multilayered structures consisting of alternating magnetic and nonmagnetic layers are investigated. In Sec. VI our model is applied to all-magnetic multilayers. Section VII summarizes the results.

II. DETAILS OF CALCULATION

We follow the continuum-type approach used by Rado and Hicken²⁰ as well as by Cochran and Dutcher,²¹ who presented results on single ferromagnetic layers for wave propagation perpendicular to the direction of the static magnetization. The magnetization was assumed to lie in the layer plane and parallel to the applied magnetic field. In the following we retain the assumption of in-plane orientation of the saturation magnetization, but allow for arbitrary in-plane angles of wave propagation. Since mode damping effects are quite weak in the wave-vector regime accessible by Brillouin light scattering, they are not considered in this paper.

The coordinate system used in the following is shown in Fig. 1. The x axis is perpendicular to the magnetic layers. For an N -layer system the positions of the interfaces

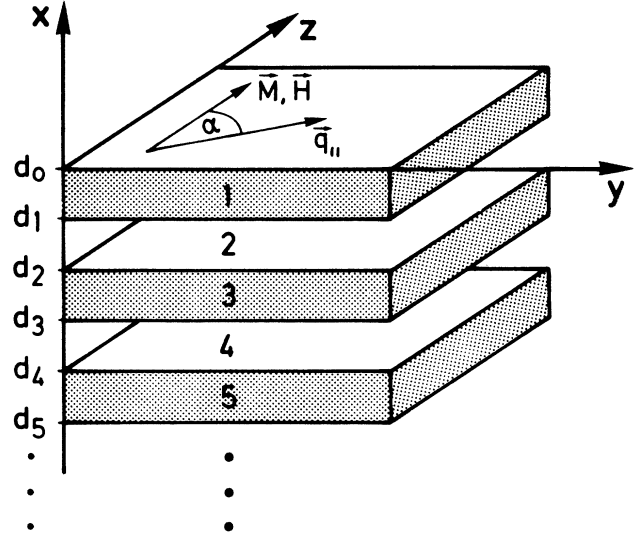


FIG. 1. Coordinate system used for calculating spin-wave frequencies. Shown is an example of a layered structure consisting of three magnetic layers, with layer indices $n=1,3,5$ and two intervening nonmagnetic layers ($n=2,4$). The positions of the interfaces are $d_n, n=0, \dots, 5$.

are defined by $d_n, n=1 \dots N$, such that for the n th layer the interfaces lie at $x=d_{n-1}$ and $x=d_n$. We use the index n to indicate parameters of the n th layer, but when appropriate this index is omitted for an improved clarity of the formulas. We assume that the applied magnetic field \mathbf{H} is collinear with the saturation magnetization $4\pi\mathbf{M}_n$ in each magnetic layer, which can be achieved for strong enough applied external fields. Without loss of generality, the external field \mathbf{H} and $4\pi\mathbf{M}_n$ in each magnetic layer are in the z direction. We define the angle Φ as the angle between $4\pi\mathbf{M}$ and a crystallographic reference direction within the film plane, which is normally [100]. The direction of the mode propagation, defined by the mode's wave-vector component parallel to the film plane, q_{\parallel} is within the (y,z) plane. Its angle with the z axis, i.e., the direction of the saturation magnetization, is α .

We begin with the full Landau-Lifshitz torque equation of motion

$$\frac{1}{\gamma} \frac{\partial \mathbf{M}}{\partial t} = \mathbf{M} \times \left[\mathbf{H} - \frac{1}{M} \nabla_{\mathbf{M}} E_{\text{ani}} + \frac{2A}{M^2} \nabla^2 \mathbf{M} \right], \quad (1)$$

where $\gamma = \gamma_e g / 2$ is the gyromagnetic ratio, $\gamma_e = 1.759 \times 10^7$ Hz/Oe is the value of γ for the free electron, and g is the spectroscopic splitting factor. E_{ani} is the usually defined magnetic volume anisotropy energy density, and A is the exchange stiffness constant. We have omitted the layer index n for clarity. Also, the magnetostatic Maxwell equations have to be fulfilled:

$$\nabla \times \mathbf{H} = 0, \quad (2)$$

$$\nabla \cdot (\mathbf{H} + 4\pi\mathbf{M}) = 0. \quad (3)$$

From the equation of motion [Eq. (1)] and the Maxwell equations [Eqs. (2) and (3)], boundary conditions can be derived. At each interface the parallel component of \mathbf{H} and the perpendicular component of $\mathbf{H} + 4\pi\mathbf{M}$ have to be continuous. From the equation of motion [Eq. (1)] we obtain the condition that the sum of the interface torques must be zero for each interface. If at the $x = d_n$ interface there is no exchange coupling to the adjacent magnetic layer, the so-called Rado-Weertman boundary condition has to be fulfilled:²³

$$\mathbf{M} \times \left[\frac{1}{M} \nabla_{\mathbf{M}} E_{\text{inter}} - \frac{2A \partial \mathbf{M}}{M^2 \partial n} \right] = 0 \Big|_{x=d_n}, \quad (4)$$

where E_{inter} is the interface anisotropy energy. $\partial/\partial n$ is the partial derivative with respect to the surface normal unit vector, $\hat{\mathbf{n}}$. The latter points from the interface into the magnetic layer. In the presence of exchange coupling between two magnetic layers, labeled with the indices n and n' , the so-called Hoffmann boundary conditions have to be fulfilled:^{24,25}

$$\mathbf{M}_n \times \left[\frac{1}{M_n} \nabla_{\mathbf{M}_n} E_{\text{inter},n} - \frac{2A_n}{M_n^2} \frac{\partial \mathbf{M}_n}{\partial n_n} \right] \Big|_{x=d_n} - \frac{2A_{nn'}}{M_n M_{n'}} \mathbf{M}_n \times \mathbf{M}_{n'} \Big|_{x=d_{n'-1}} = 0 \quad (5)$$

$$\mathbf{M}_{n'} \times \left[\frac{1}{M_{n'}} \nabla_{\mathbf{M}_{n'}} E_{\text{inter},n'} - \frac{2A_{n'}}{M_{n'}^2} \frac{\partial \mathbf{M}_{n'}}{\partial n_{n'}} \right] \Big|_{x=d_{n'-1}} - \frac{2A_{nn'}}{M_n M_{n'}} \mathbf{M}_{n'} \times \mathbf{M}_n \Big|_{x=d_n} = 0. \quad (6)$$

For interfaces between two magnetic layers n' is given by $n' = n + 1$, whereas for exchange coupling across a (thin) nonmagnetic layer $n' = n + 2$. The interlayer exchange constant between layer n and n' is $A_{nn'}$. Without loss of generality we call this parameter A_{12} in the following. The interface normal, $\hat{\mathbf{n}}_n$, points into layer n , i.e., $\hat{\mathbf{n}}_n = -\hat{\mathbf{n}}_{n'}$. The first term in Eqs. (5) and (6) is the Rado-Weertman boundary condition, whereas the second term describes the exchange coupling between the two layers. Two limiting cases of the interlayer exchange constant A_{12} should be considered. For $A_{12} = 0$ Eqs. (5) and (6) resemble the Rado-Weertman boundary conditions, i.e., the interface torque densities must be zero on each side of the interface separately. For large values of A_{12} , i.e., $A_{12} \gg A_i (\partial \mathbf{M}_i / \partial n_i)$, the first term in Eqs. (5) and (6) can be neglected and we obtain simply $\mathbf{M}_n \times \mathbf{M}_{n'} = 0$, i.e., \mathbf{M}_n and $\mathbf{M}_{n'}$ are aligned either parallel or antiparallel. The interface anisotropy constant E_{inter} is defined by

$$E_{\text{inter}} = K_s u_x^2 + K_{sp} u_y^2, \quad (7)$$

where K_s is the out-of-plane interface anisotropy constant and K_{sp} the in-plane interface anisotropy constant, respectively. The direction cosines of \mathbf{M} , in the coordinate system described above are u_x and u_y .

We now turn to the calculation of the spin-wave frequencies. We assume that the fluctuations in \mathbf{M} and \mathbf{H} associated with the spin waves are small compared to the static values. This condition is almost always fulfilled for thermally driven spin waves at temperatures considerably less than T_c .²⁶ We split \mathbf{M} and \mathbf{H} into frequency-independent static parts \mathbf{M}_0 and \mathbf{H}_0 and dynamic parts \mathbf{m} and \mathbf{h} :

$$\mathbf{M}(t) = \mathbf{M}_0 + \mathbf{m}(t), \quad |\mathbf{m}| \ll |\mathbf{M}_0|, \quad (8)$$

$$\mathbf{H}(t) = \mathbf{H}_0 + \mathbf{h}(t), \quad |\mathbf{h}| \ll |\mathbf{H}_0|. \quad (9)$$

In principle we have to find the static equilibrium orientations of the magnetizations for the layered system be-

fore calculating the spin-wave frequencies. Due to interface anisotropies and exchange coupling effects the static equilibrium direction might differ from the bulk direction. The direction of magnetization can be obtained by solving the equation of motion [Eq. (1)] and the magnetostatic Maxwell equations [Eqs. (2) and (3)] with the appropriate boundary condition [Eqs. (4)–(6)] for time-independent \mathbf{M} and \mathbf{H} .²⁷ It should be noted that in the general case the direction of the magnetization is a function of the position in each magnetic layer. Once we have solved the static problem all time-independent terms contained in Eqs. (1)–(6) cancel to zero.

Let us define $\mathbf{q} = (q_x, q_y, q_z)$ as the spin-wave wave vector, and q_{\parallel} (q_{\perp}) as the component of \mathbf{q} parallel (perpendicular) to the interfaces. Thus $q^2 = q_x^2 + q_y^2 + q_z^2$, $q_{\parallel}^2 = q_y^2 + q_z^2$, and $q_{\perp} = q_x$. In a Brillouin light scattering experiment q_{\parallel} , and thus $q_y = q_{\parallel} \sin \alpha$ and $q_z = q_{\parallel} \cos \alpha$, are defined by the scattering geometry due to wave-vector conservation in the scattering process. We assume that inside the ferromagnetic film \mathbf{h} and \mathbf{m} are proportional to

$$\exp[i(\omega t - q_x x - q_y y - q_z z)].$$

Outside the film \mathbf{h} is proportional to

$$\exp[i(\omega t - q_y y - q_z z) - q_x^2 x],$$

and \mathbf{m} is zero. Using Eqs. (8) and (9) we linearize Eqs. (1)–(6) by dropping all terms that are of quadratic or of higher order in components of \mathbf{m} and \mathbf{h} . We assume that the magnetization lies along its equilibrium direction. Thus the equation of motion [Eq. (1)] is a homogeneous system of linear equations in the components of \mathbf{m} and \mathbf{h} :

$$-q_z h_y + q_y h_z = 0, \quad (10)$$

$$-q_y h_x + q_x h_y = 0, \quad (11)$$

$$q_x h_x + q_y h_y + q_z h_z + 4\pi q_x m_x + 4\pi q_y m_y + 4\pi q_z m_z = 0, \quad (12)$$

$$Mh_y + \frac{i\omega}{\gamma} m_x - \left[H + H_\beta + 2 \frac{A}{M} q^2 \right] m_y = 0, \quad (13)$$

$$-Mh_x + \left[H + H_\alpha + \frac{2A}{M} q^2 \right] m_x + \frac{i\omega}{\gamma} m_y = 0, \quad (14)$$

$$\frac{i\omega}{\gamma} m_z = 0, \quad (15)$$

with

$$H_\alpha m_x = M \frac{dE_{\text{ani}}}{dm_x}, \quad (16)$$

$$H_\beta m_y = M \frac{dE_{\text{ani}}}{dm_y}, \quad (17)$$

where H_α and H_β are the anisotropy fields. For (001) surfaces of cubic systems these fields are given by

$$H_\alpha = \frac{K_1}{M} (2 - 16 \sin^2 \Phi + 16 \sin^4 \Phi), \quad (18)$$

$$H_\beta = \frac{K_1}{M} (2 - 4 \sin^2 \Phi + 4 \sin^4 \Phi), \quad (19)$$

and for (110) surfaces by

$$H_\alpha = \frac{K_1}{M} (2 - 7 \sin^2 \Phi + 3 \sin^4 \Phi), \quad (20)$$

$$H_\beta = \frac{K_1}{M} (2 - 13 \sin^2 \Phi + 12 \sin^4 \Phi), \quad (21)$$

with K_1 being the cubic volume anisotropy constant. From Eq. (15) it follows that m_z is zero for nonzero ω . In order that Eqs. (10)–(15) have a nontrivial solution the secular determinant of their coefficients must vanish. Neglecting the unphysical solution $q_y = 0$, the solutions are given by the zeros of the relation:

$$\left[\frac{2A}{M} \right]^2 q^6 + \frac{2A}{M} (4\pi M + 2H + H_\alpha + H_\beta) q^4 + \left[(H + H_\alpha)(4\pi M + H + H_\beta) - 8\pi A q_z^2 - \left[\frac{\omega}{\gamma} \right]^2 \right] q^2 + 4\pi M [(H_\beta - H_\alpha) q_\parallel^2 - (H + H_\beta) q_z^2] = 0. \quad (22)$$

Since q_\parallel and q_z are constants defined by the scattering geometry and the wave number of the incident light, Eq. (22) is the dispersion relation between the spin-wave frequency ω and the wave-vector component perpendicular to the layers, $q_\perp = q_x$. We label the six roots of q_\perp by $q_{x1} \dots q_{x6}$. The calculations of these quantities are performed numerically. The corresponding dynamic fields and magnetizations are labeled h_{xi} , h_{yi} , m_{xi} , and m_{yi} , respectively, for $i = 1, \dots, 6$.

For an easier analysis of the boundary conditions it is convenient to express h_{yi} , m_{xi} , and m_{yi} in terms of h_{xi} . From Eq. (11) we find

$$h_{yi} = \frac{q_y}{q_{xi}} h_{xi}. \quad (23)$$

For m_{xi} and m_{yi} we define the quantities u_i and v_i

$$m_{xi} = u_i h_{xi}, \quad (24)$$

$$m_{yi} = v_i h_{xi}. \quad (25)$$

From Eqs. (13) and (14) we are able to calculate the quantities u_i and v_i :

$$u_i = M \frac{H + H_\alpha + \frac{2A}{M} q_i^2 - (i\omega/\gamma)(q_\parallel \sin \alpha / q_{xi})}{[H + H_\alpha + (2A/M) q_i^2][H + H_\beta + (2A/M) q_i^2] - (\omega/\gamma)^2}, \quad (26)$$

$$v_i = M \frac{[H + H_\beta + (2A/M) q_i^2](q_\parallel \sin \alpha / q_{xi}) + i\omega/\gamma}{[H + H_\alpha + (2A/M) q_i^2][H + H_\beta + (2A/M) q_i^2] - (\omega/\gamma)^2}. \quad (27)$$

In the nonmagnetic layers we obtain from Eq. (2) and (3)

$$iq_\parallel h_x^e - q_x^e h_\parallel^e = 0, \quad (28)$$

$$q_x^e h_x^e + iq_\parallel h_\parallel^e = 0, \quad (29)$$

where h_\parallel is the component of \mathbf{h} in the direction of q_\parallel . A nonvanishing solution of Eqs. (28) and (29) requires

$$q_x^e = \pm q_\parallel, \quad (30)$$

where we label the two solutions of Eq. (30) by q_{x1}^e and q_{x2}^e . We then obtain

$$h_\parallel^{e+} = ih_{x1}^e, \quad (31)$$

$$h_\parallel^{e-} = -ih_{x2}^e. \quad (32)$$

Outside the layers we must require $h_{x2}^e = 0$ for the vacuum above the layers and $h_{x1}^e = 0$ for the vacuum below

the layers, respectively, since h_x^e must approach zero for $x \rightarrow \pm \infty$.

We now turn to the boundary conditions, which mix the six solutions for h_{xi} , h_{yi} , m_{xi} , and m_{yi} at the interfaces d_n . Continuity of h_{\parallel} and of $h_x + 4\pi m_x$ requires

$$\sum_{i=1}^6 \frac{q_{\parallel}}{q_{xi}} h_{xi} e^{-iq_{xi}d_n} - i h_{x1}^e e^{-q_{\parallel}d_n} + i h_{x2}^e e^{q_{\parallel}d_n} = 0, \quad (33)$$

$$\sum_{i=1}^6 (1 + 4\pi u_i) h_{xi} e^{-iq_{xi}d_n} - h_{x1}^e e^{-q_{\parallel}d_n} - i h_{x2}^e e^{q_{\parallel}d_n} = 0, \quad (34)$$

for magnetic/nonmagnetic interfaces, and

$$\sum_{i=1}^6 \frac{q_{\parallel}}{q_{xi,n}} h_{xi,n} e^{-iq_{xi,n}d_n} - \sum_{i=1}^6 \frac{q_{\parallel}}{q_{xi,n+1}} h_{xi,n+1} e^{-iq_{xi,n+1}d_n} = 0, \quad (35)$$

$$\sum_{i=1}^6 (1 + 4\pi u_{i,n}) h_{xi,n} e^{-iq_{xi,n}d_n} - \sum_{i=1}^6 (1 + 4\pi u_{i,n+1}) h_{xi,n+1} e^{-iq_{xi,n+1}d_n} = 0, \quad (36)$$

for magnetic/magnetic interfaces. The Rado-Weertman boundary condition [Eq. (4)] reads:

$$\sum_{i=1}^6 (K_s - K_{sp} \cos^2 \Phi \mp i A q_{xi}) u_i h_{xi} e^{-iq_{xi}d_n} = 0, \quad (37)$$

$$\sum_{i=1}^6 [K_{sp} (1 - 2 \cos^2 \Phi) \mp i A q_{xi}] v_i h_{xi} e^{-iq_{xi}d_n} = 0, \quad (38)$$

where \mp refers, respectively, to the upper or lower interface of the magnetic layer. For coupling between two magnetic layers with interfaces at $x = d_n$ and $x = d_{n'-1}$ we obtain from the Hoffmann boundary conditions [Eqs. (5) and (6)]

$$\sum_{i=1}^6 (-i A_n q_{xi,n} + K_{s,n} - K_{sp,n} \cos^2 \Phi + A_{nn'}) u_{i,n} h_{xi,n} e^{-iq_{xi,n}d_n} - \sum_{i=1}^6 \frac{M_{n'}}{M_n} A_{nn'} u_{i,n} h_{xi,n'} e^{-iq_{xi,n'}d_{n'}} = 0, \quad (39)$$

$$\sum_{i=1}^6 [-i A_n q_{xi,n} + K_{sp,n} (1 - 2 \cos^2 \Phi) + A_{nn'}] v_{i,n} h_{xi,n} e^{-iq_{xi,n}d_n} - \sum_{i=1}^6 \frac{M_{n'}}{M_n} A_{nn'} v_{i,n} h_{xi,n'} e^{-iq_{xi,n'}d_{n'}} = 0, \quad (40)$$

$$\sum_{i=1}^6 (i A_n q_{xi,n} + K_{s,n} - K_{sp,n} \cos^2 \Phi + A_{nn'}) u_{i,n} h_{xi,n} e^{-iq_{xi,n}d_n} - \sum_{i=1}^6 \frac{M_n}{M_{n'}} A_{nn'} u_{i,n} h_{xi,n'} e^{-iq_{xi,n'}d_{n'}} = 0, \quad (41)$$

$$\sum_{i=1}^6 [i A_n q_{xi,n} + K_{sp,n} (1 - 2 \cos^2 \Phi) + A_{nn'}] v_{i,n} h_{xi,n} e^{-iq_{xi,n}d_n} - \sum_{i=1}^6 \frac{M_n}{M_{n'}} A_{nn'} v_{i,n} h_{xi,n'} e^{-iq_{xi,n'}d_{n'}} = 0, \quad (42)$$

where $A_{nn'}$ is the interlayer exchange constant between layer n and n' . Equation (33)–(42) form a system of linear equations in $h_{xi,n}$ or h_{xi}^e , respectively. Since there are six solutions to h_{xi} in each magnetic layer, two solutions h_{xi}^e in each nonmagnetic layer, and two solutions outside the multilayer, the dimension of the system of linear equations is given by $2 + 6N_{\text{mag}} + 2N_{\text{nonmag}}$, where N_{mag} (N_{nonmag}) is the total number of magnetic (nonmagnetic) layers. In order to fulfill the boundary conditions simultaneously for all interfaces, the determinant of the system of linear equations must equal zero. For finding the spin-wave frequencies the numerical procedure is as follows: For a given frequency ω Eqs. (22), (26), and (27) are used to calculate $q_{xi,n}$, $u_{i,n}$, and $v_{i,n}$. Then the value of the boundary condition determinant is evaluated. In a root finding routine ω is varied and the boundary condition determinant is calculated until the value of the boundary condition determinant fulfills a convergence criterion. The calculations are performed by means of appropriate numerical tools. In the following sections examples are presented on spin-wave calculations in single magnetic layers, magnetic double layers and magnetic/nonmagnetic as well as all-magnetic multilayered structures.

III. SINGLE MAGNETIC FILMS

The first results on spin-wave calculations in single magnetic films, based on the aforementioned theory, were reported by Rado and Hicken²⁰ for Fe(110) films for propagation in the [001] direction and by Cochran and Dutcher²¹ for Fe(001) films for propagation in the [100] direction. Both dipolar modes (Damon-Eshbach modes) and exchange modes (so-called standing spin waves) are contained in the model. In the cross-over regime of dipolar modes and exchange modes, these modes show repulsions and mix their mode characters. In the presence of interface anisotropies, as is the case in, e.g., epitaxial Fe films, the frequency of the dipolar mode diverges for film thickness approaching zero. In this section we call interface anisotropies “surface anisotropies”, which is more convenient for single films.

Figure 2 shows the calculated spin-wave frequencies for Fe(110) as a function of the film thickness. The propagation direction is [001], and the applied magnetic field is 1 kG. The film parameters, listed in the figure caption, are taken from a fit to experimental data.¹² The latter were obtained from an *in situ* Brillouin light scattering experiment on epitaxially grown Fe(110) films on a

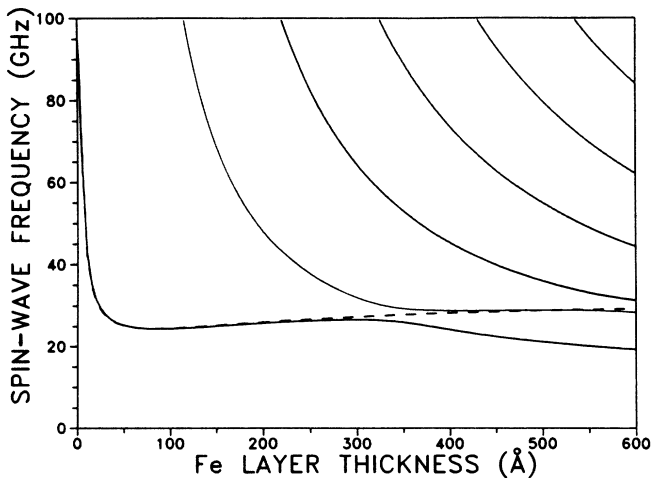


FIG. 2. Spin-wave frequencies as a function of layer thickness for a single-crystal Fe(110) layer. The full lines are a calculation with the theory described in the text; the dashed line is an effective-volume-anisotropy approach neglecting exchange contributions. The parameters are: $4\pi M = 18$ kG, $H = 1$ kG, $g = 2.1$, $A = 2 \times 10^{-6}$ erg/cm, $K_1 = 4.8 \times 10^5$ erg/cm³, $K_s = 2.8$ erg/cm², $K_{sp} = 0.024$ erg/cm², $q_{||} = 1.73 \times 10^5$ cm⁻¹.

W(110) substrate.¹² The full line is the calculation using the theory described in the previous section. For comparison the broken line shows the calculation using a simplified approach, in which surface anisotropies are treated as effective volume anisotropies and exchange contributions are neglected.^{12,13} Of course the latter approach can only yield the dipolar mode. For the dipolar mode the agreement of both calculations is quite good, since exchange contributions to the dipolar mode are relatively small.

Figure 3 shows the frequencies of the dipolar mode (lowest-frequency mode) and the first exchange modes for a 200-Å thick Fe film as a function of the in-plane angle Φ .

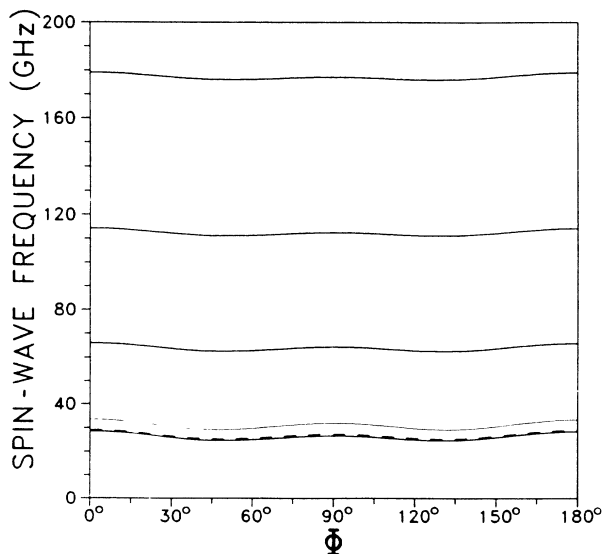


FIG. 3. Spin-wave frequencies as a function of the in-plane angle Φ . The parameters are as in Fig. 2.

Φ between the direction of magnetization and the [100] axis, i.e., on rotating the sample about the film normal. The surface anisotropy constant K_s is 2.8 erg/cm². Not only the dipolar mode but also the first exchange modes are significantly affected by changing the orientation of the magnetization with respect to the crystallographic axes. For comparison, the calculation based on the same parameter set using a simplified approach neglecting exchange is shown by the dashed line.

We now focus on the separate influence of the surface anisotropies of both film sides on the spin-wave frequencies. In our approach surface anisotropies, described by an out-of-plane component K_s and an in-plane component K_{sp} , enter via the Rado-Weertman boundary condition [Eq. (4)]. Thus, surface anisotropies can be studied separately for each surface. Treating surface anisotropies as effective volume anisotropies (i.e., dividing the surface anisotropy energy by the film thickness and adding this to the volume-anisotropy energy density term) does not allow the separation of the contributions from the two surfaces, since only the averaged values of both the surface anisotropies enter the effective anisotropy energy density. The effect of different surface anisotropies on both sides of the film is to slightly change the spin-wave frequency upon reversal of the propagation direction, or equivalently, upon reversal of the externally applied magnetic field. The results from our calculations are shown in Fig. 4 for a 10-Å thick Fe(110) film. The change in spin-wave frequency upon reversal of either $q_{||}$ on H is plotted as a function of the difference of the out-of-plane surface anisotropy constant K_s between the two surfaces. The averaged value of K_s in erg/cm² is indicated on each curve. First of all, the frequency difference is linearly proportional to the difference in K_s between both sides of the film. Thus, a high-resolution Brillouin light scatter-

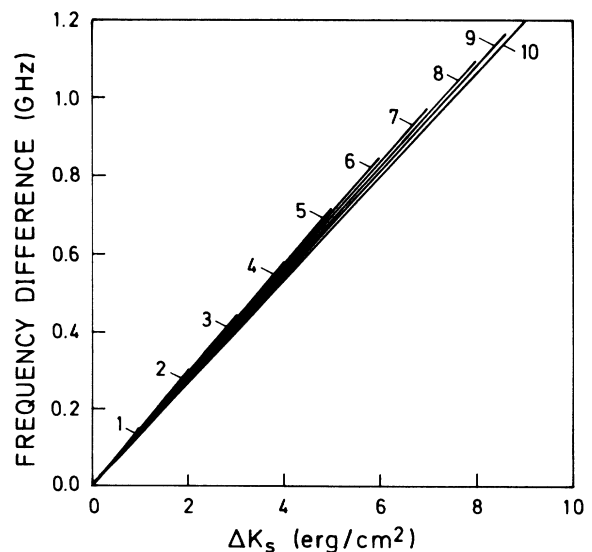


FIG. 4. Change in spin-wave frequencies upon reversal of $q_{||}$ as a function of the difference in the out-of-plane surface anisotropies of both film sides for a 10-Å thick Fe layer. $H = 1$ kG, $4\pi M = 21$ kG, the other parameters are as in Fig. 2. The sum of K_s of both film sides is indicated at each graph.

ing experiment should be directly able to determine the difference in K_s between both film sides. This would provide important information on, e.g., the epitaxial growth properties of the film on a given substrate. Second, the frequency difference is rather insensitive to the absolute value of K_s . A detailed study shows that this is also true for a large range of film thickness, of saturation magnetization, and of applied magnetic field. Although the effect is quite small, high-resolution Brillouin scattering experiments should be able to confirm these results.

IV. MAGNETIC DOUBLE LAYERS

Magnetic double layers are an important model system to study the coupling mechanisms between two magnetic films in close contact. In addition to dipolar coupling, the exchange coupling mechanism becomes important if the distance between the two magnetic films is closer than the exchange coupling length, which is of the order of a few Ångströms. Experimentally, there exist a number of reports by Grünberg and co-workers on Fe, Co, and Permalloy double layers with Au, Cr, Cu, and Pd as the spacer layer materials.^{16,28} Varying the spacer layer thickness, the exchange coupling of the two magnetic films was varied and its influence on the spin-wave modes studied. In the case of Cr, antiferromagnetic coupling between the two magnetic films was also observed.

Based on the aforementioned theoretical approach, there are reports from three groups in which the spin-wave modes were calculated for magnetic double layers.^{10,14-18} Since the spacer layer thickness, which is typically of the order of 2–20 Å, is much smaller than the magnetic film thickness, it can be neglected for the calculation of the spin-wave frequencies. In this case the layer system is described by two magnetic layers in contact. For the interface the Hoffmann boundary conditions Eqs. (5) and (6) have to be used. The interlayer exchange coupling is described by the interlayer exchange constant A_{12} . Figure 5 shows a calculation of the spin-wave frequencies as a function of the interlayer exchange constant A_{12} for two 400 Å Fe layers in contact. For zero interlayer exchange the films are only dipolar coupled. The dipolar mode at 33.2 GHz is the Damon-Eshbach mode of an 800-Å thick Fe film. The three modes at 15.4, 23.3, and 41.4 GHz are the exchange modes of a single 400 Å layer, since these modes in the two layers do not interact. The insets of Fig. 5 show the fluctuating parts of the magnetization component perpendicular to the films as a function of the position in the layers. The center horizontal line is at $m_{\perp}=0$. The center vertical line indicates the interface between the two layers. The Damon-Eshbach mode of the double-layer system still shows the characteristic decay of the amplitude of m_{\perp} from one surface to the other. The exchange modes are characterized by the increasing number of nodes in the magnetization profile. The discontinuity in m_{\perp} at the interface is much larger for the exchange modes than for the dipolar mode due to the absence of exchange coupling at the interface. With increasing interlayer exchange constant A_{12} the degeneracy of the exchange modes in the two layers is lifted and each exchange mode splits into a symmetriclike and

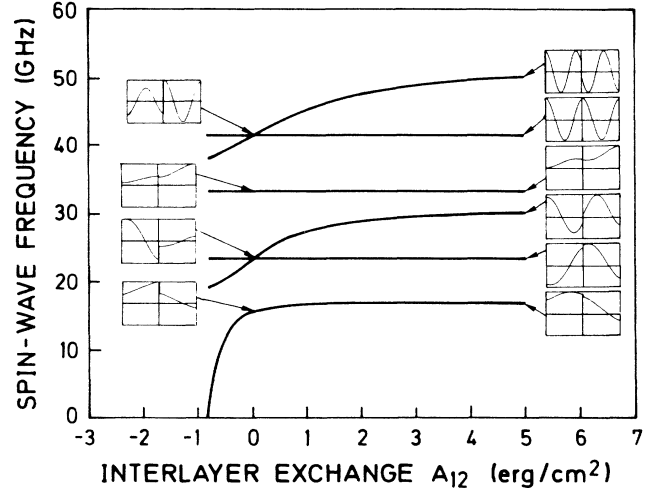


FIG. 5. Spin-wave frequencies as a function of the inter-layer exchange coupling constant A_{12} for a double layer consisting of two 400 Å Fe layers in an applied magnetic field of 1 kG. The insets show the perpendicular component of the fluctuating part of the magnetization as a function of the position in the film stack.

an antisymmetriclike mode with respect to the interface. [We use the expression “(anti)symmetriclike,” since the symmetry is slightly broken by the presence of the dipolar interaction.] With increasing A_{12} the frequencies of the symmetric modes do not change significantly, since the mode frequencies for $A_{12}=0$ are already close to those of the even-numbered exchange modes of an 800-Å thick film. The frequencies of the antisymmetriclike modes increase and converge to the exchange-mode frequencies of the odd-numbered exchange modes of an 800 Å thick film. For $A_{12}=5$ erg/cm² the frequencies of the modes shown in Fig. 5 seem to be close to the full coupling limit. It is noteworthy that for this value A_{12} is still much smaller than in the full coupling limit, which can be estimated as $A_{12}^c = 2A/a$ for bcc and fcc lattices, where a is the lattice parameter. For Fe this estimate for A_{12}^c is of the order of 100 erg/cm². The magnetization profiles show that at the interface the discontinuities in m_{\perp} are much smaller than for $A_{12}=0$, but still finite. Since for exchange modes the Brillouin light scattering cross section is very dependent on the net fluctuating magnetic moment, the mode intensities in a Brillouin spectrum can still be expected to be very sensitive to A_{12} in this regime. However, a detailed calculation of the scattering cross section is beyond the scope of this paper. For $A_{12} \approx -0.8$ erg/cm² the lowest-order exchange mode becomes soft and goes to zero. This indicates a transition of the equilibrium state of the magnetization of the system from parallel to antiparallel alignment of the magnetizations of the two films.

V. MAGNETIC/NONMAGNETIC MULTILAYERS

Magnetic/nonmagnetic multilayered structures have received considerable attention in the past due to novel

magnetic excitations, which only exist in these types of artificial structures. Due to a coupling of the dipolar surface spin-wave modes (Damon-Eshbach modes) of each magnetic layer across the intervening nonmagnetic spacer layers, their frequency degeneracy is lifted. These coupled modes show partial surface-modelike as well as bulk-modelike behavior. In the limit of many bilayers they form a band of collective spin-wave excitations. In the dipolar limit these modes have been studied both theoretically and experimentally. In this paper we include both bulk exchange as well as interlayer exchange contributions and, in particular, we study the cross-over regime of dipolar modes with the exchange modes.

We consider the case of a multilayer stack consisting of single-crystal Fe(110) layers separated by nonmagnetic layers of equal thickness. This structure resembles Fe/Pd superlattices, where the Fe crystallites have preferred (110) orientation,¹³ as well as single-crystal epitaxial Fe films on W(110) substrates.¹² For the simulations, the parameters of the latter are used for the saturation magnetization and the out-of-plane interface anisotropy constant K_s . The parameters are listed in the figure captions of this section. The value of the in-plane interface constant $K_{sp} = 0.024$ erg/cm² has been dropped because it does not affect the spin-wave frequencies in the layer-thickness regime considered here. The wave-vector points in the [001] direction, and the applied magnetic field is 1 kG.

Figure 6 shows calculated spin-wave frequencies as a function of the single-layer thickness for a multilayered structure consisting of five bilayers. The thickness d of the magnetic layers equals that of the nonmagnetic layers. Two kinds of modes are observed. Between about

18–35 GHz there are five dipolar modes (Damon-Eshbach modes) separated in frequency because of the dipolar interaction across the nonmagnetic layers. They are intersected by, and hybridized with, exchange modes at about $d = 350, 600,$ and 850 Å. The frequency splitting of the dipolar modes decreases with increasing d because of a corresponding decrease in the interlayer coupling. For very small layer thicknesses ($d < 30$ Å) the dipolar modes exhibit a characteristic increase in frequency because interface anisotropy contributions become dominant in this regime. The highest-frequency mode is the Damon-Eshbach surface spin-wave mode of the total multilayer stack. For $d \rightarrow 0$, all modes but the highest-frequency mode become degenerate. An analysis shows that, as a result of the dominating interface anisotropies, the dipolar mode in each layer becomes bulk modelike, with minor stray fields in the spacer layers, thus exhibiting reduced coupling. For $d > 250$ Å, the range of dipolar modes is crossed by the exchange modes. The latter are characterized by their typical $1/d^2$ behavior. Their stray fields in the spacer layers are very weak, resulting in virtually no mode splitting apart from the crossing regime. For small layer thicknesses, a weak but still significant dependence of the exchange-mode frequencies on the interface anisotropy constants was established. In the crossing regime, the dipolar modes and the exchange modes mix their mode type, leading to a pronounced frequency gap. Although in this thickness regime the energetic contributions of the interface anisotropies are very small, the gap width is determined primarily by K_s . This is demonstrated in Fig. 7, where the spin-wave frequencies are plotted for $d = 630$ Å (indicated by the dashed

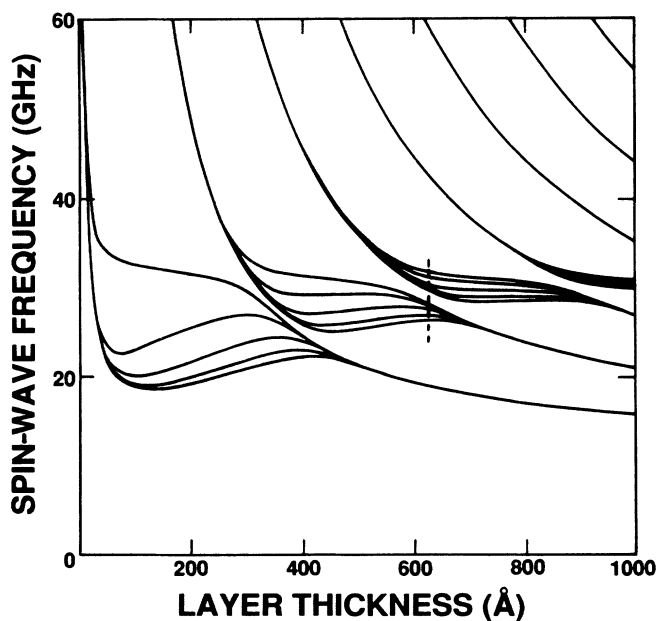


FIG. 6. Spin-wave frequencies as a function of single-layer thickness for a multilayer consisting of five layers of Fe(110) and interleaving nonmagnetic layers of same thickness. The parameters are as in Fig. 2. The dashed line indicates the thickness position referred to by Fig. 7.

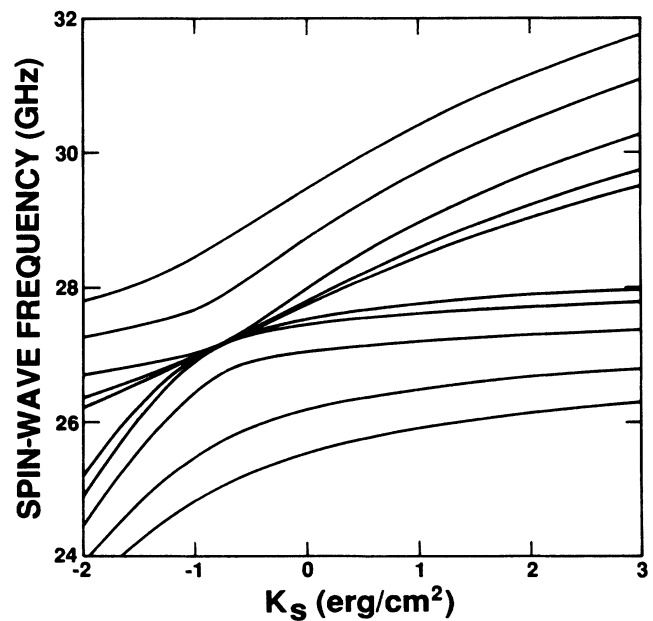


FIG. 7. Spin-wave frequencies as a function of the out-of-plane interface anisotropy constant K_s for a magnetic/nonmagnetic multilayer as in Fig. 6 for $d = 630$ Å (as indicated in Fig. 6).

line in Fig. 6) as a function of the interface anisotropy constant K_s . For negative values of K_s , the gap width shrinks virtually to zero and then increases for even smaller values of K_s . A study of the form of the dispersion curves as a function of the number of bilayers N reveals no strong dependence of the gap width on N . However, because of numerical instabilities, N could not be chosen larger than about ten. An extrapolation of the results implies that the properties of the crossing regime, in particular the gap width and the importance of interface anisotropies, are much the same for larger N , i.e., superlattices.

An important issue is the possible role of interlayer exchange coupling in magnetic/nonmagnetic multilayers. Due to the short range of interlayer exchange coupling it can significantly contribute only for very small thicknesses (a few atomic layers) of the nonmagnetic spacer layers. Fig. 8 shows calculated spin-wave frequen-

cies as a function of the single-layer thickness d for a magnetic/nonmagnetic multilayer consisting of five double layers. The thickness of the magnetic layers equals that of the nonmagnetic layers. For the exchange coupling constant A_{12} it is assumed that A_{12} is proportional to $\exp(-d/d_0)$ with d the thickness of the nonmagnetic spacer layer and d_0 a characteristic decay length ($d_0 = 10$ Å in Fig. 8). For $d > 60$ Å, interlayer exchange is negligible and we obtain the spin-wave properties as described earlier. The first single-layer exchange mode with its characteristic $1/d^2$ thickness behavior can be seen on Fig. 8 for $d > 100$ Å. For very small layer thicknesses all of the coupled dipolar modes but the highest-frequency dipolar mode show a very strong frequency increase and cross the highest-frequency dipolar mode. In the crossing regime a very small mode repulsion is found, which can hardly be resolved in Fig. 8. For comparison, the mode behavior for $A_{12} = 0$ is plotted as dashed lines in Fig. 8.

From these obtained properties we are now able to draw some important analogies between bulk- and surface-spin-wave properties in (bulk) single layers and in multilayers. For a single magnetic layer there exists one dipolar surface mode nearly unaffected by exchange. The bulk spin waves, which contain both dipolar and exchange contributions, are frequency shifted to high frequencies and become the so-called standing spin-waves since, due to the finite film thickness and the associated large wave-vector component perpendicular to the film, exchange contributions become dominant. For a magnetic/nonmagnetic multilayer the role of volume exchange interaction is replaced by interlayer exchange. For large spacer thicknesses, the latter can be neglected and we are left with the purely dipolar coupled modes. For small spacer thicknesses the onset of interlayer exchange converts all but one of the dipolar modes into exchange-dominated modes. The remaining dipolar mode is essentially a surface mode of the total multilayer stack. Thus, as a basic conclusion, magnetic/nonmagnetic multilayered structures can be regarded as a model system to study the basic coupling mechanisms of dipolar modes with suppressed exchange interaction.

VI. ALL-MAGNETIC MULTILAYERS

In the case of all-magnetic multilayered structures, i.e., alternating magnetic films with different magnetic parameters such as saturation magnetization, g factor, or interface anisotropies, the spin-wave modes of each magnetic layer are coupled to those of adjacent layers both by the dipolar coupling mechanism as well by interlayer exchange. For studying the latter effect, all-magnetic multilayers seem to be a good test system due to both the multiple number of interfaces as well as the specific properties of the coupled modes spectra.²² Pure exchange coupling between magnetic layers has been investigated by ferromagnetic resonance.^{5,7,29,30} However, in the present study dipolar coupling also is included.

As a model system we consider a multilayer stack consisting of three Fe layers of equal thickness interleaved by two Ni layers of the same thickness. The system Fe/Ni is

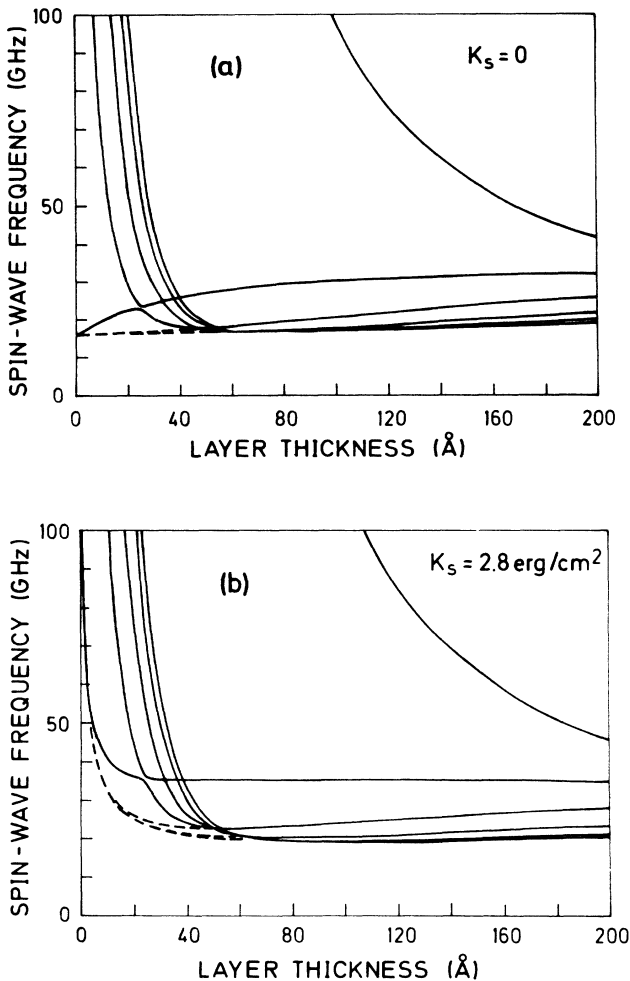


FIG. 8. Spin-wave frequencies for a magnetic/nonmagnetic multilayer, as in Figs. 6 and 7, as a function of single-layer thickness. The full lines are a calculation including interlayer exchange interaction across the nonmagnetic layers. The dashed lines are calculations without interlayer coupling. $A_{12}(d_0=0) = 10$ erg/cm², $d_0 = 10$ Å. (a) $K_s = 0$; (b) $K_s = 2.8$ erg/cm².

of specific interest since, coincidentally, the lowest-lying exchange modes of both materials are nearly identical in frequency for the same single-layer thickness. Figure 9 shows the calculated spin-wave frequencies as a function of the single-layer thickness. The parameters used are the bulk literature values of the saturation magnetization, the g factor and the exchange constant of Fe and Ni. The interlayer exchange coupling constant A_{12} has been chosen to be $A_{12} = 10 \text{ erg/cm}^2$. Interface anisotropies have been set to zero; calculations using nonzero values exhibited modifications close to those discussed in the preceding sections. The most striking feature in Fig. 9 is the lifting of the degeneracy for the exchange modes. With the exception of the lowest two modes, the observed exchange modes always can be subdivided into groups of five modes, and each group can be further subdivided into a two-mode and a three-mode subgroup. Each subgroup corresponds to a single-layer exchange mode for either Fe or Ni. For the lowest-lying group the single-layer Fe exchange mode and the corresponding Ni exchange mode are nearly degenerate, as shown by the nearly equal spacing of all five modes. In the limit of an infinite number of layers (superlattice structure) the modes eventually form a band of collective exchange modes, similar to the band of collective dipolar modes in magnetic/nonmagnetic-type superlattices. The frequency splitting of the exchange modes strongly depends on the interlayer exchange constant A_{12} . This is demonstrated in Fig. 10, where the spin-wave frequencies are plotted as a function of the interlayer exchange constant A_{12} . The Fe and Ni layer thickness is 100 \AA . For $A_{12} = 0$ there are three dipolar-type modes, two of which are doubly degenerate. With increasing A_{12} four of them become exchange dominated, the fifth mode is the dipolar stack surface mode, which is insensitive to exchange. These properties are close to those calculated for magnetic/nonmagnetic multilayers, except that we are now dealing with two different kinds of magnetic materials. At about 100 GHz

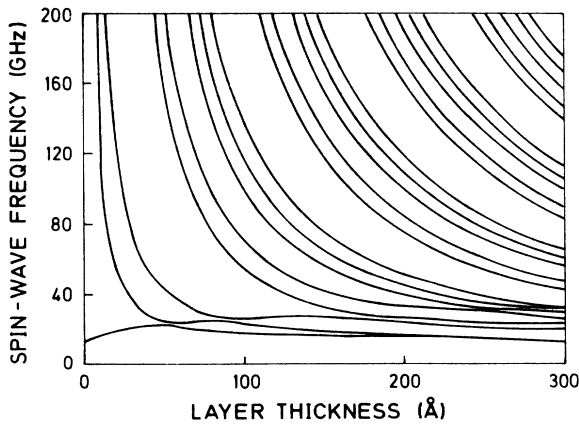


FIG. 9. Spin-wave frequencies as a function of single-layer thickness for an Fe/Ni/Fe/Ni/Fe multilayer structure. The parameters are Fe: $4\pi M = 21 \text{ kG}$, $g = 2.1$, $A = 2 \times 10^{-6} \text{ erg/cm}$; Ni: $4\pi M = 6 \text{ kG}$, $g = 2.2$, $A = 0.7 \times 10^{-6} \text{ erg/cm}$. The applied magnetic field is 1 kG , the interlayer exchange constant is $A_{12} = 10 \text{ erg/cm}^2$.

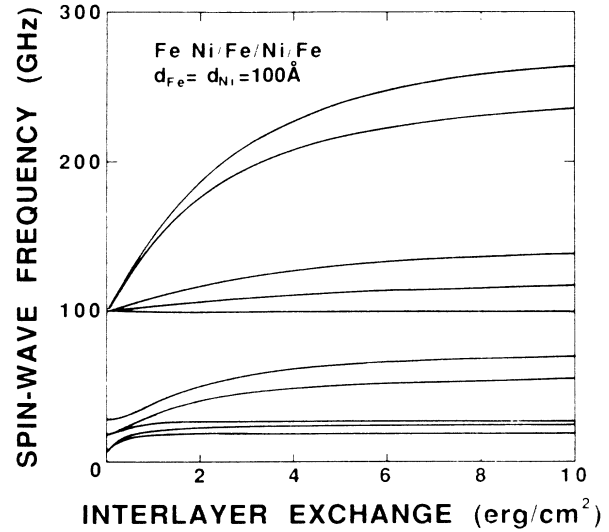


FIG. 10. Spin-wave frequencies as a function of the interlayer exchange constant A_{12} for a multilayer structure, as in Fig. 9.

the exchange mode of Fe, and just above 100 GHz the exchange mode of Ni, can be observed. The Fe exchange modes as well as the Ni exchange modes are degenerate in frequency, since their dipolar stray fields are extremely weak in the adjacent layers. With increasing interlayer exchange the exchange modes become coupled and split into three Fe modes and two Ni modes. Of particular interest is that with increasing interlayer exchange the Ni modes show a strong mode repulsion from the Fe modes, which increases their frequencies much more than the frequency splitting due to the lift of degeneracy. For $A_{12} \rightarrow \infty$ the Ni modes approach the Fe exchange modes of next higher order, and both show a nearly equidistant mode separation.

VII. CONCLUSIONS

Results are presented in this paper for propagating spin waves in single ferromagnetic layers, double layers, as well as for magnetic/nonmagnetic and all-magnetic multilayered structures. With only the restrictions of in-plane orientation of the saturation magnetizations in each layer and their collinearity with the applied magnetic field, the model presented here can be applied to a large number of layered ferromagnetic structures. The variety of magnetic bulk and interface mechanisms that determine the spin-wave properties of these materials opens a large field of possible spin-wave excitations, with use for the determination of magnetic parameters as well as possible applications, e.g., in data processing using magnetic devices.

For single magnetic films both dipolar and exchange dominated modes are calculated. Surface anisotropies strongly influence the spin-wave frequencies for small film thicknesses. For nonzero wave vectors, different surface anisotropies on each side of the film imply changes in the spin-wave frequencies upon inversion of the propagation direction. The latter opens potential applications in the field of surface magnetism. For magnetic/

nonmagnetic multilayers, collective dipolar modes have been calculated and their crossing with the exchange-dominated modes has been investigated. The gap width in the crossing regime is mainly determined by the amount of interface anisotropy. For very thin spacer thicknesses, where magnetic interlayer coupling across nonmagnetic layers becomes important, all but the highest-frequency dipolar coupled modes become a new type of exchange modes. In the case of all-magnetic multilayered structures, a new type of collective spin waves (i.e., coupled exchange modes) are observed, reminiscent of dipolar collective spin-wave excitations in magnetic/nonmagnetic superlattices. The mode splitting of these collective spin waves depends strongly on the interlayer exchange constant A_{12} . It should be highly feasible to test all these predictions by means of Brillouin light scattering experiments, with the potential of gaining new ways for evaluating multilayer-specific properties.

ACKNOWLEDGMENTS

I would like to thank Professor G. I. Stegeman at Optical Sciences Center, University of Arizona, Tucson, Arizona for his hospitality and continuing support at the Optical Sciences Center, where large parts of the current work have been performed, and Professor G. Güntherodt for discussions and continuing support. Discussions at different stages of the project with Professor G. T. Rado, Professor R. E. Camley, Dr. P. Grünberg, Dr. J. Barnás, Dr. J. R. Dutcher, Dr. R. L. Stamps, and P. Baumgart are gratefully acknowledged. I would like to thank Professor C. M. Falco for a critical reading of the manuscript. Part of this work was supported by the Air Force Office of Scientific Research/University Research Initiative Program under Contract No. F49620-86-C-0123, as well as by Deutsche Forschungsgemeinschaft, Sonderforschungsbereich (SFB) 125 and 341.

- ¹R. E. Camley, T. S. Rahman, and D. L. Mills, *Phys. Rev. B* **27**, 261 (1983).
²P. Grüberg and K. Mika, *Phys. Rev. B* **27**, 2955 (1983).
³P. R. Emtage and M. R. Daniel, *Phys. Rev. B* **29**, 212 (1984).
⁴G. Rupp, W. Wettling, and W. Jantz, *Appl. Phys. A* **42**, 45 (1987).
⁵R. P. van Staple, F. J. A. M. Greidanus, and J. W. Smits, *J. Appl. Phys.* **57**, 1282 (1985).
⁶L. Dobrzynski, B. Djafari-Rouhani, and H. Puzkarski, *Phys. Rev. B* **33**, 3251 (1986).
⁷E. L. Albuquerque, P. Fulco, E. F. Sarmiento, and D. R. Tilley, *Solid State Commun.* **58**, 41 (1986).
⁸L. L. Hinchey and D. L. Mills, *Phys. Rev. B* **33**, 3329 (1986).
⁹K. Vayhinger and H. Kronmüller, *J. Magn. Magn. Mater.* **62**, 159 (1986).
¹⁰K. Vayhinger and H. Kronmüller, *J. Magn. Magn. Mater.* **72**, 307 (1986).
¹¹J. Barnás, *J. Phys. C* **21**, 1021 (1988); **21**, 4097 (1988).
¹²B. Hillebrands, P. Baumgart, and G. Güntherodt, *Phys. Rev. B* **36**, 2450 (1987).
¹³B. Hillebrands, A. Boufelfel, C. M. Falco, P. Baumgart, G. Güntherodt, E. Zirngiebl, and J. D. Thompson, *J. Appl. Phys.* **63**, 3880 (1988).
¹⁴P. Grünberg, R. Schreiber, Y. Pang, M. B. Brodsky, and H. Sowers, *Phys. Rev. Lett.* **57**, 2442 (1986).
¹⁵F. Saurenbach, U. Walz, L. L. Hinchey, P. Grünberg, and W.

- Zinn, *J. Appl. Phys.* **36**, 2442 (1986).
¹⁶M. Vohl, J. Barnás, and P. Grünberg (unpublished).
¹⁷B. Heinrich, S. T. Purcell, J. R. Dutcher, K. B. Urquhart, J. F. Cochran, and A. S. Arrott (unpublished).
¹⁸J. F. Cochran and J. R. Dutcher, *J. Appl. Phys.* **64**, 6092 (1988).
¹⁹M. Grimsditch, M. R. Khan, and I. K. Schuller, *Phys. Rev. Lett.* **51**, 498 (1983).
²⁰G. T. Rado and R. J. Hicken, *J. Appl. Phys.* **63**, 3885 (1988).
²¹J. F. Cochran and J. R. Dutcher, *J. Appl. Phys.* **63**, 3814 (1988).
²²B. Hillebrands, *Phys. Rev. B* **37**, 9885 (1988).
²³G. T. Rado and J. R. Weertman, *J. Phys. Chem. Solids* **11**, 315 (1959).
²⁴F. Hoffmann, A. Stankoff, and H. Pascard, *J. Appl. Phys.* **41**, 1022 (1970).
²⁵F. Hoffmann, *Phys. Status Solidi* **41**, 807 (1970).
²⁶This requirement is not fulfilled if the effective internal field, i.e., the sum of the external field, the demagnetizing field, and the anisotropy fields, is close to zero.
²⁷G. T. Rado, *Phys. Rev. B* **26**, 295 (1982).
²⁸F. Saurenbach, J. Barnás, G. Binasch, M. Vohl, P. Grünberg and W. Zinn (unpublished).
²⁹C. Vittoria, *Phys. Rev. B* **32**, 1679 (1985).
³⁰S. W. McKnight and C. Vittoria, *Phys. Rev. B* **36**, 8574 (1987).

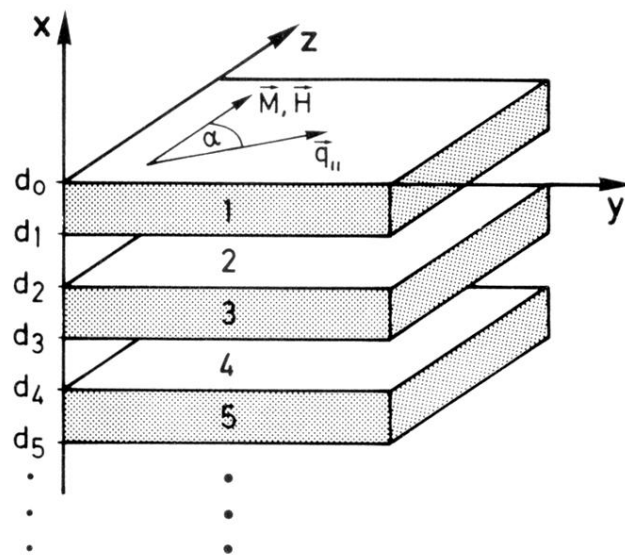


FIG. 1. Coordinate system used for calculating spin-wave frequencies. Shown is an example of a layered structure consisting of three magnetic layers, with layer indices $n=1,3,5$ and two intervening nonmagnetic layers ($n=2,4$). the positions of the interfaces are $d_n, n=0, \dots, 5$.